Inflammation, Vol. 43, No. 1, February 2020 (© 2019)
DOI: 10.1007/s10753-019-01125-8

ORIGINAL ARTICLE

Piceatannol Inhibits *P. acnes*–Induced Keratinocyte Proliferation and Migration by Downregulating Oxidative Stress and the Inflammatory Response

Tingting Zhu,[1] Fumin Fang,[1] Dongjie Sun,[2] Shuyun Yang,[3] Xiaoping Zhang,[1] Xiuqin Yu,[1,5] and Li Yang[4,5]

Abstract— The *Cutibacterium acnes* (also called *Propionibacterium acnes*, *P. acnes*)-induced proliferation and migration of keratinocytes contribute to acne vulgaris (AV), which is a common inflammatory skin disease that causes physical and psychological impairments. Piceatannol (3, 5, 3′, 4′-tetrahydroxy-trans-stilbene, PCT) is naturally present in many human diets and plays antioxidant and anti-inflammatory roles that inhibit cell proliferation and migration. We aimed to analyse the functions and underlying mechanisms of PCT in *P. acnes*-stimulated keratinocytes. First, PCT showed no toxicity against the normal human keratinocyte cell line HaCaT but inhibited *P. acnes*-induced HaCaT cell proliferation. Next, PCT promoted the nuclear translocation and target gene transcription of the antioxidant transcription factor nuclear factor erythroid 2-related factor 2 (Nrf2), thereafter decreasing intracellular reactive oxygen species (ROS) levels. In addition, PCT inhibited the nuclear translocation of p65 [a subunit of nuclear factor kappa B (NF-κB)] and the secretion of pro-inflammatory cytokines, including interleukin-6 (IL-6), tumour necrosis factor-α (TNF-α) and interleukin-8 (IL-8). Finally, a transfection assay showed that PCT inhibited *P. acnes*-induced HaCaT cell proliferation and migration by activating the antioxidant Nrf2 pathway and inhibiting the inflammatory NF-κB pathway. Our data suggested that PCT alleviated *P. acnes*-induced HaCaT cell proliferation and migration through its antioxidant and anti-inflammatory roles, suggesting the potential of PCT to treat AV.

KEY WORDS: acne vulgaris; *Propionibacterium acnes*; Piceatannol; nuclear factor erythroid 2-related factor 2; anti-inflammation.

Tingting Zhu, Fumin Fang, Xiuqin Yu and Li Yang contributed equally to this work.

[1] Department of Dermatology, The First Affiliated Hospital of Soochow University, No.188, Shizi Street, Suzhou, 215006, China
[2] Department of Dermatology, First Affiliated Hospital of Kunming Medical University, Kunming, 650032, China
[3] Department of Dermatology, The People's Hospital of Baoshan, Baoshan City, 678000, China
[4] Department of Dermatology, Henan Provincial People's Hospital, The People's Hospital of Zhengzhou University, Zhengzhou, 450000, China
[5] To whom correspondence should be addressed to Xiuqin Yu at Department of Dermatology, The First Affiliated Hospital of Soochow University, No.188, Shizi Street, Suzhou, 215006, China. E-mail: syuxiuqin2010@163.com; and Li Yang at Department of Dermatology, Henan Provincial People's Hospital, The People's Hospital of Zhengzhou University, Zhengzhou, 450000, China. E-mail: yangli180409@163.com

INTRODUCTION

Acne vulgaris (AV) is a common inflammatory skin disease, impacting approximately 10% of the total population worldwide [28]. AV undoubtedly decreases the quality of life of patients because AV not only affects appearance but also causes psychological problems, such as depression, anxiety and self-abasement [42]. The pathogenesis of AV is extremely complex and undefined, mainly comprising the following four aspects: hkeratinization of the pilosebaceous duct, *Cutibacterium acnes* (also named *Propionibacterium acnes*, *P. acnes*) and inflammation [10, 24].

The human skin, the largest organ of the body, contains numerous vital microbial genera related to skin health, including *Staphylococcus*, *Propionibacterium*, *Streptococcus*, *Corynebacterium* and *Malassezia* [28]. In particular, the gram-positive anaerobic bacterium *P. acnes* is an important component of the normal human skin microbiota and controls pilosebaceous units. However, *P. acnes* is not always beneficial to the human body. Of the cutaneous propionibacteria, *P. acnes* appears to be the most frequent cause of opportunistic infection and is linked to AV. Higher antibody titres to AV are observed in patients with severe forms of acne than in healthy individuals [32]. Moreover, highly complex *P. acnes* macrocolonies or biofilms appear to be a more common phenomenon in AV than in normal skin samples; thus, we speculate that these structures could impede sebum flow [19]. *In vitro*, *P. acnes* induces oxidative stress [15] and the inflammatory response [22] in keratinocytes, consequently promoting cell proliferation and migration [20], which facilitate the progression of AV [12].

Piceatannol (3, 5, 3′, 4′-tetrahydroxy-trans-stilbene; PCT) is a natural stilbene derived from plant seeds [27]. PCT acts as an antioxidant agent by activating the Kelch-like ECH-associated protein 1 (Keap1)/nuclear factor erythroid 2-related factor 2 (Nrf2)/antioxidant response element (ARE) pathway. Nrf2 is a kind of transcription factor that regulates many ARE-containing genes involved in the antioxidant response, thus protecting cells against reactive oxygen species (ROS)/reactive nitrogen species (RNS) to maintain cellular redox homeostasis [25]. KEAP1 constitutively binds and suppresses Nrf2 activity under normal conditions, while oxidants block the KEAP1-mediated proteasomal degradation of Nrf2, which leads to increased nuclear translocation and, in turn, the transcriptional induction of target genes that ensure cell survival [8]. PCT also plays an anti-inflammatory role by inhibiting the nuclear factor kappa B (NF-κB) pathway [26]. In mammals, NF-κB is composed of homo- and heterodimers of five members of the Rel family, namely, NF-κB1 (p105/p50), NF-κB2 (p100/p52), RelA (p65), RelB and c-Rel. *P. acnes* activates NF-κB and promotes the nuclear translocation of NF-κB. Subsequently, NF-κB upregulates the transcription of a range of pro-inflammatory cytokines, such as interleukin-6 (IL-6), tumour necrosis factor-α (TNF-α) and interleukin-8 (IL-8), enhancing the inflammatory response [39]. Additionally, PCT inhibits the proliferation and migration of multiple normal and cancer cells, including human aortic smooth muscle cells [9], mouse mammary cancer [34] and rat hepatocyte carcinoma [23]. However, the functions and mechanisms of PCT in the proliferation and migration of keratinocytes are unclear.

In this study, we aimed to analyse the functions and underlying mechanisms of PCT in *P. acnes*-stimulated keratinocytes. Our data suggested that PCT alleviated *P. acnes*-induced HaCaT cell proliferation and migration *via* its antioxidant and anti-inflammatory roles, suggesting the potential of PCT to treat AV.

MATERIALS AND METHODS

HaCaT Cell Culture and Treatment

Human keratinocyte cells (HaCaT cell line) were purchased from the American Type Culture Collection (#CRL-1624; ATCC, Rockville, MD, USA). HaCaT cells were cultured in high-glucose Dulbecco's modified Eagle's medium (DMEM) (Gibco, Life Technologies, Carlsbad, CA, USA) supplemented with 10% fetal bovine serum (FBS), penicillin (100 U/ml), streptomycin (100 mg/ml) and glutamine (2 mM) (all from Gibco) and maintained in a humidified atmosphere at 37 °C with 5% CO_2. The cells were sub-cultured every 4–6 days or when they reached 80–90% confluency. For the treatment, 2.0×10^4–1.2×10^5 HaCaT cells/ml seeded on 96- and 6-well microplates depending on the assay and cultured for 24 h before treatment. HaCaT cells were pre-exposed to 10^5, 10^6, 10^7 or 10^8 CFU/ml of heat-killed *P. acnes* for 24 h. PCT (#P0453; purity > 95%; Sigma Aldrich, St. Louis, MO, USA) was dissolved in dimethyl sulfoxide (DMSO) before use, and its chemical structure is shown in Fig. 1a. HaCaT cells were treated with PCT at concentrations of 0, 5, 10, 15 or 20 μM for 24 h (Fig. 1b). In the other experiments, HaCaT cells were treated with PCT at a concentration of 15 μM for 24 h. For the study of nuclear factor kappa B (NF-κB) pathway, the NF-κB inhibitor JSH-23 (J4455,

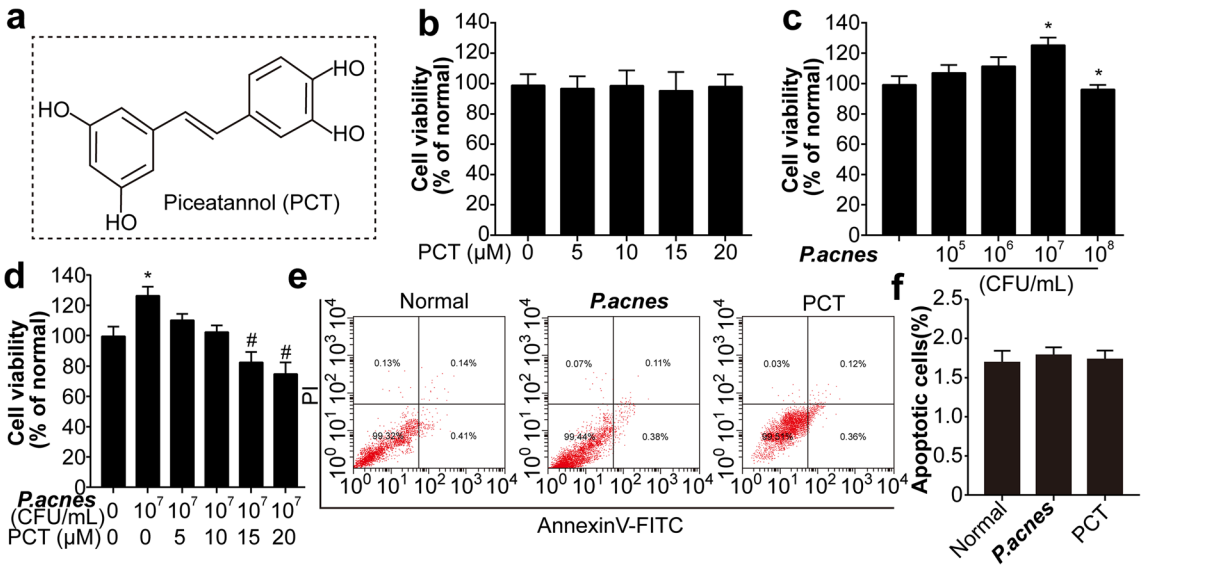

Fig. 1. PCT shows no toxicity against normal HaCaT cells and inhibits *P. acnes*-induced cell proliferation. **a** The molecular structure of PCT is shown. **b** HaCaT cells were treated with PCT at the concentration of 0 (normal group), 5, 10, 15 or 20 μM for 24 h. Then, a CCK-8 assay was performed to detect cell viability. **c** HaCaT cells were treated with *P. acnes* at the concentration of 0 (normal group), 10^5, 10^6, 10^7 or 10^8 CFU/ml for 24 h. Then, a CCK-8 assay was performed to detect cell viability. $^*P < 0.05$ vs. the normal group. **d** HaCaT cells were randomly divided into the following six groups and treated without or with *P. acnes* at a concentration of 10^7 CFU/ml: no *P. acnes* + no PCT (normal group), *P. acnes*, *P. acnes* + 5 μM PCT, *P. acnes* + 10 μM PCT, *P. acnes* + 15 μM PCT and *P. acnes* + 20 μM PCT. Then, a CCK-8 assay was performed to detect cell viability. $^*P < 0.05$ vs. the normal group; $\#P < 0.05$ vs. the *P. acnes* group. The cell viability in the normal group was considered to be 100%, and the cell viability in other groups was calculated as the average ratio relative to the normal group. **e** Cell apoptosis was measured after treating cells for 24 h with 10^7 CFU/ml *P. acnes* or 15 μM PCT treatment. The flow cytometry profile represents Annexin V-FITC staining on the X-axis and PI on the Y-axis. Numbers represent the percentage of cells in each quadrant. **f** The statistical analysis of cell apoptosis ratio in normal, *P. acnes* and PCT groups.

Merck, USA) was used to treat HaCaT cells at the concentration of 10 μM for 24 h.

Cell Viability Assay

Cell Counting Kit-8 (CCK-8; Dojindo Laboratories, Japan) was applied to quantify cell viability. HaCaT cells were seeded in 96-well plates with 100 μl of medium at a density of 2×10^4 cells/well. After incubation of cells with intended reagents, 10 μl of CCK8 solution was added to each well and incubated for 1 h at 37 °C. Finally, the absorbance values at 450 nm were determined by a microplate reader (ELX800, BioTek Instruments, Winooski, VT, USA) [41].

Cell Apoptosis Assay Using Annexin-V/PI Staining and Flow Cytometry

Apoptosis was quantified using the fluorescein isothiocyanate (FITC) -Annexin V Apoptosis Detection Kit (556547, BD Biosciences Pharmingen, USA). After treatment without or with 10^7 CFU/ml PA, or 15 μM PCT for 24 h, HaCaT cells were harvested and suspended in Annexin binding buffer (2×10^6 cells/200 ml). Subsequently, HaCaT cells were incubated with Annexin V-FITC and propidium iodide (PI) for 15 min at room temperature in the dark and immediately analysed by the Gallios flow cytometer with Kaluza software (Beckman Coulter Inc. USA). Annexin V negative/PI positive cells were assumed to be necrotic (right lower quadrant), Annexin V positive/PI positive cells were considered as late apoptotic (right upper quadrant) and Annexin V positive/PI negative cells were assumed to be early apoptotic cells (left upper quadrant).

Western Blot Analysis

After treatment, HaCaT cells were washed three times with cold phosphate-buffered saline (PBS). Then, the cells were lysed in radio-immunoprecipitation assay (RIPA) lysis buffer supplemented with phosphatase inhibitor and protease inhibitor cocktails (Sigma-Aldrich) for 30 min on ice. After centrifugation at 12,000×*g* for 20 min at 4 °C, the supernatant was obtained as the total protein extract. A nuclear and cytoplasmic protein extraction kit (Beyotime, Shanghai, China) was used to isolate the nuclear protein

from HaCaT cells according to the manufacturer's instructions. Protein concentrations were determined by a BCA protein assay kit (Thermo Fisher, Madison, WI, USA). Protein samples were fractionated with 10% sodium dodecyl sulfate polyacrylamide gel electrophoresis (SDS-PAGE) and then transferred to a polyvinylidene difluoride (PVDF) membrane (Bio-Rad Laboratories, Hercules, USA). After blocking with 5% (weight/volume; *w*/*v*) nonfat milk in Tris-buffered saline containing 0.1% Tween-20 (0.1% TBST) for 2 h at room temperature, the membrane was incubated with primary antibodies overnight at 4 °C and horseradish peroxidase (HRP)-conjugated secondary antibodies for 2 h at room temperature. The primary antibodies used in the study, including anti-Nrf2 (#ab137550), anti-KEAP1 (#ab119403), anti-haem oxygenase 1 (HO-1) (#ab13243), anti-quinone oxidoreductase 1 (NQO1) (#ab34173), anti-p65 (#ab16502), anti-histone 3 (H3) (#ab18521) and anti-β-actin (#ab8227), were from Abcam (Cambridge, MA, USA). Protein bands were visualized by using a chemiluminescence reagent and analysed with a Bio-Rad imaging system (Bio-Rad Laboratories, Hercules, CA, USA).

Immunofluorescent Staining of HaCaT Cells

HaCaT cells were fixed with a 4% paraformaldehyde (PFA)-PBS solution for 24 h, washed with PBS and permeabilized with 0.5% Triton-X100. Cells were immunostained with anti-Nrf2 (Abcam). Alexa Fluor 488 anti-rabbit IgG (#A27034; Thermo Fisher Scientific, Waltham, MA, USA) was used as a secondary antibody. Cell nuclei were visualized with 4′, 6-diamidino-2-phenylindole dihydrochloride (DAPI; #D1306; Thermo Fisher Scientific) staining. The fluorescent staining was visualized with a laser scanning confocal microscope (Olympus, Tokyo, Japan) at 40× magnification.

HaCaT Cell Transfection

Nrf2 siRNAs (Nrf2 siRNA1-3), pEGFP-N1-p65 and scrambled siRNA were purchased from Genema (Shanghai, China). HaCaT cells were transfected with 100 nM Nrf2 siRNAs and scrambled siRNA using Hiperfect transfection reagent (QIAGEN, GmbH, Hilden, Germany) following the manufacturer's instructions and transfected with 50 nM pEGFP-N1-p65 using Lipofectamine 3000 (Invitrogen, Carlsbad, CA, USA).

Intracellular ROS Detection Assay

Intracellular ROS was quantified by 2′, 7′-dichlorodihydoro-fluorescein diacetate (DCFH-DA) (#D6883; Sigma Aldrich). DCFH-DA is a cell permeable lipophilic compound that can be deacetylated in the presence of cellular esterases, and the resulting 2′, 7′-dichlorodihydoro-fluorescein (DCFH) is oxidized to fluorescent 2′, 7′-dichlorofluorescein (DCF) in the cytoplasm [2]. HaCaT cells were seeded in a 6-well plate at a density of 1×10^5. Cells were incubated with or without HDC and GDH-HDC for 24 h and then washed with phenol Dulbecco's phosphate-buffered saline (DPBS). DCFH-DA at 5 μM was added to each well and further incubated at 37 °C for 0.5 h. The cells were observed under a laser scanning confocal microscope (Olympus).

Enzyme-Linked Immunosorbent Assay (ELISA)

Human IL-6 (#D6050), TNF-α (#DTA00D) and IL-8 (#D8000C) Quantikine ELISA kits were purchased from R&D (Nivelles, Belgium). The HaCaT cell culture supernatant was added to a microtitre plate coated with monoclonal antibody (Quantikine) directed against the specific cytokines and incubated at room temperature for 2 h with continuous shaking. After washing the unbound protein, polyclonal (Quantikine) antibodies directed against the respective cytokines was added for 1-h incubation period. After several washes, a substrate solution composed of hydrogen peroxide and chromogen was added to the wells. The reaction was stopped by the addition of a stop solution (H_2SO_4). Colour intensity was measured by the absorbance at 450 nm. According to the manufacturer, the minimum detectable concentrations were 0.7 pg/ml for IL-6, 5.5 pg/ml for TNF-α and 7.5 pg/ml for IL-8. The intra-assay coefficients of variation for the cell culture supernatant assay were 0.7–3.1% for IL-6, 4.4–5.3% for TNF-α and 4.4–4.7% for IL-8. The inter-assay coefficients of variation for the cell culture supernatant assay were 2–3.7% for IL-6, 6.8–8.7% for TNF-α and 5.2–8.8% for IL-8.

Ethynyl Deoxyuridine (EdU) Assay

HaCaT cell proliferation was measured using EdU kits (RiboBio, Guangzhou, China) according to the manufacturer's instructions to analyse the incorporation of EdU during DNA synthesis. The average ratio of EdU-positive cells to DAPI-positive cells was calculated.

Scratch Wound Healing Assay

HaCaT cells (70–80% confluence, cultured for 24 h) were seeded on a 24-well tissue culture plate and randomly divided into the following eight groups: normal, *P. acnes*, *P. acnes* + Nrf2 siRNA3, *P. acnes* + JSH-23 (5 μM, 30 min

prior to imaging; #S7351; Selleck Chemicals, Houston, TX, USA), *P. acnes* + PCT, *P. acnes* + Nrf2 siRNA3 + PCT, *P. acnes* + pEGFP-N1-p65 + PCT and *P. acnes* + Nrf2 siRNA3 + pEGFP-N1-p65 + PCT. Next, cell culture monolayers were scratched with a sterile 200-μl pipette tip across the centre of the well. After scratching, the wells were gently washed twice with PBS to remove the detached cells. Three hundred microlitres of DMEM was added to each well and photographed using a camera attached to inverted microscope to obtain the same field during the image acquisition; markings were created to use as reference points close to the scratch. The wound gap was imaged at the 24 h time point to check the wound width of different treatments. Scratch wound closure was viewed using an inverted microscope, and images were captured with a digital camera (Nikon Coolpix 4500; Nikon, Tokyo, Japan). Images were analysed by Carl Zeiss Microscopy GmbH software by monitoring the width of the scratch area at the 24 h time point.

Statistical Analysis

All data are displayed as the mean ± SD based on at least three replicates. The differences between groups were analysed by a Student's *t* test, with $P < 0.05$ considered statistically significant.

RESULTS

PCT Shows No Toxicity Against Normal HaCaT Cells and Inhibits *P. Acnes*-Induced Cell Proliferation

First, we wondered whether PCT had certain side effects and showed that PCT had no effect on normal HaCaT cell proliferation (Fig. 1b). Following stimulation with *P. acnes*, HaCaT cell proliferation increased in a concentration-dependent manner, peaking at the concentration of 10^7 CFU/ml, which was chosen for subsequent experiments (Fig. 1c). Additionally, PCT inhibited *P. acnes*-induced HaCaT cell proliferation in a concentration-dependent manner (Fig. 1d). HaCaT cell apoptosis was not up-regulated by PCT, indicating the absence of cellular toxicity for PCT (Fig. 1e, f). The data suggested that PCT alleviated *P. acnes*-induced HaCaT cell proliferation.

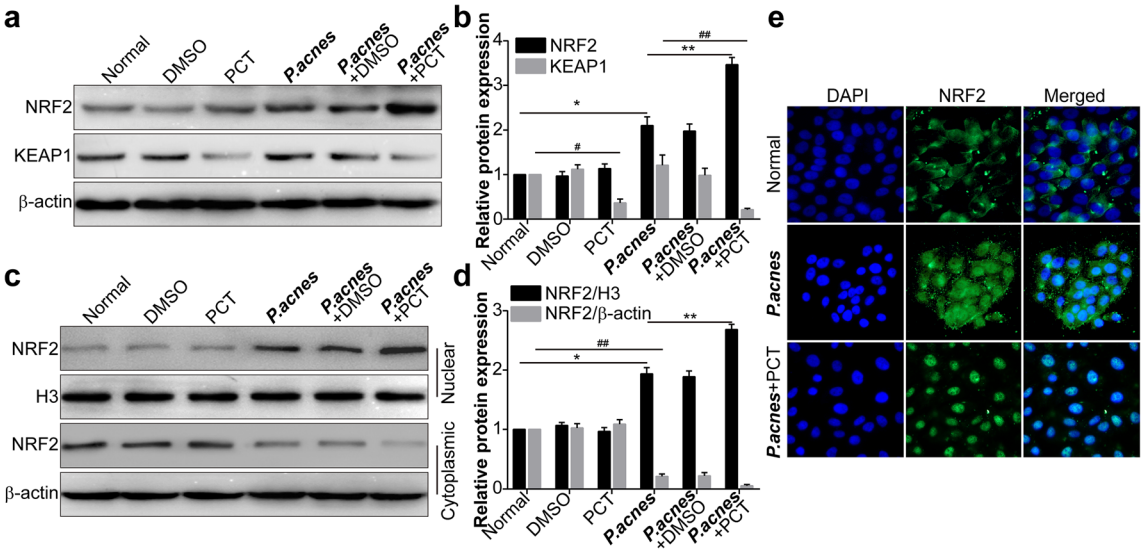

Fig. 2. -0.2pt?>PCT promotes Nrf2 expression and nuclear translocation. HaCaT cells were randomly assigned to one of six groups: normal, DMSO, PCT (15 μM), *P. acnes* (10^7 CFU/ml), *P. acnes* + DMSO and *P. acnes* + PCT. **a** Western blot analysis was performed to detect Nrf2 and KEAP1 protein levels. β-actin was used as the loading control. **b** Statistical analysis of the relative protein levels of Nrf2 and KEAP1. $^{\#}P < 0.05$ vs. relative protein level of KEAP1 in the normal group. $^{*}P < 0.05$ vs. relative protein level of Nrf2 in the normal group. $^{***}P < 0.005$ vs. relative protein level of Nrf2 in the *P. acnes* group. $^{\#\#}P < 0.01$ vs. relative protein level of KEAP1 in the *P. acnes* group. **c** Nuclear and cytoplasmic separation and Western blot analysis were performed to detect Nrf2 subcellular location. H3 and β-actin were used as the nuclear and cytoplasmic loading controls, respectively. **d** Statistical analysis of Nrf2 relative protein levels. $^{*}P < 0.05$, $^{**}P < 0.01$ vs. relative protein level of Nrf2 in the normal group. $^{\#\#}P < 0.01$, $^{\#\#\#}P < 0.005$ vs. relative protein level of KEAP1 in the normal group. **e** HaCaT cells were randomly divided into three groups, normal, *P. acnes* and *P. acnes* + PCT, and then, the cells were stained with DAPI (blue) and anti-Nrf2 antibody (green).

PCT Promotes Nrf2 Expression and Nuclear Translocation

Previous studies have revealed that PCT exerts an anti-oxidant effect by activating the Nrf2 pathway [33, 37]. We also found that PCT increased Nrf2 expression and decreased KEAP1 expression under *P. acnes* stimulation, without any changes under normal conditions (Fig. 2a, b). Additionally, PCT increased the nuclear translocation of Nrf2 under *P. acnes* stimulation (Fig. 2c–e) but did not affect the nuclear translocation of Nrf2 under normal conditions (Fig. 2c, d). The data suggested that PCT promoted Nrf2 expression and nuclear translocation after *P. acnes* stimulation.

PCT Plays an Anti-oxidative Role *via* the Nrf2 Pathway

We further investigated whether the anti-oxidative role of PCT was dependent on the Nrf pathway. Nrf2 siRNA3 showed the best knockdown efficiency; thus, it was applied in the subsequent experiments (Fig. 3a, b). The antioxidant molecules HO-1 [4] and NAD (P) H:NQO1 [18] are two target genes of Nrf2. Following *P. acnes* stimulation, HO-1 and NQO1 expressions were increased, while PCT further upregulated HO-1 and NQO1 expression. Interestingly, Nrf2 knockdown alleviated the PCT-induced upregulation of HO-1 and NQO1 expression (Fig. 3c, d). *P. acnes* induced ROS production in HaCaT cells, while PCT relieved oxidative stress, which was reversed by Nrf2 knockdown (Fig. 3e). The data suggested that PCT alleviated *P. acnes*-induced oxidative stress *via* Nrf2 and its target genes.

PCT Plays an Anti-inflammatory Role in *P. Acnes*-Challenged HaCaT Cells

PCT shows anti-inflammatory functions in multiple cells and diseases, such as mast cell-mediated allergic inflammation [24]. Furthermore, PCT inhibits tumour

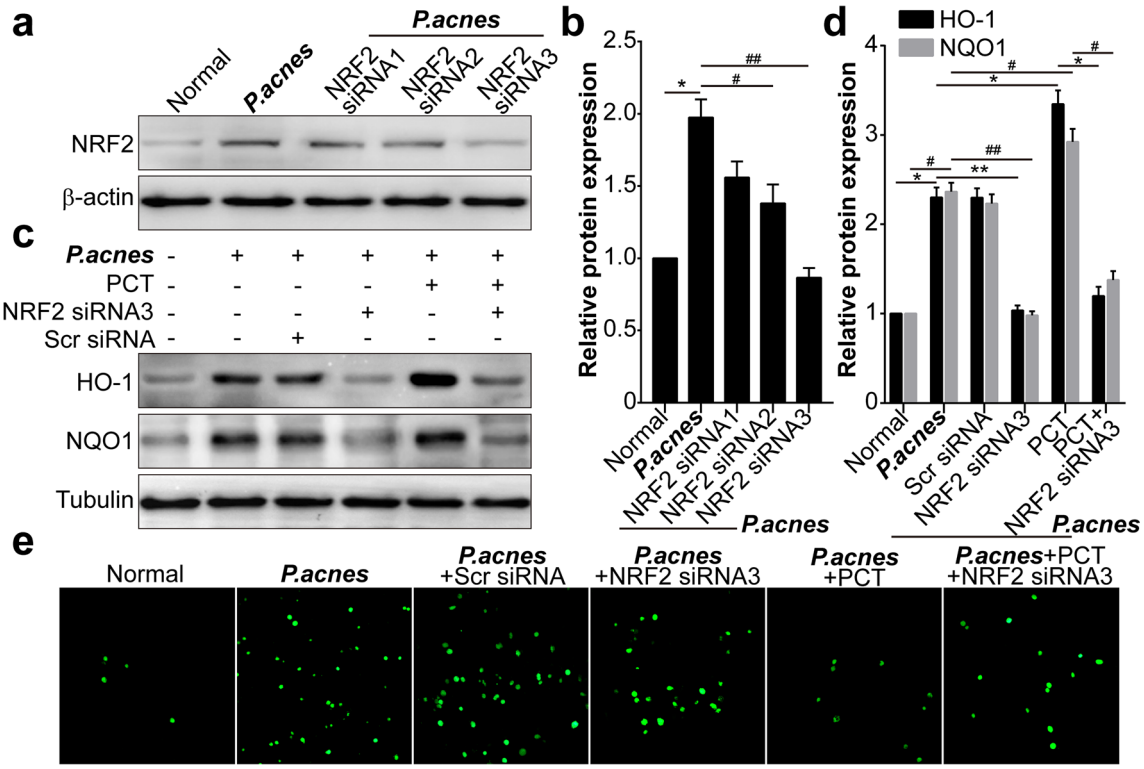

Fig. 3. PCT plays an anti-oxidative role via the Nrf2 pathway. **a** HaCaT cells were randomly assigned to one of the following five groups: normal, *P. acnes*, *P. acnes* + Nrf2 siRNA1, *P. acnes* + Nrf2 siRNA2 and *P. acnes* + Nrf2 siRNA3. Western blotting was performed to detect the Nrf2 protein level. β-actin was used as the loading control. **b** Statistical analysis of Nrf2 relative protein levels. $^{*}P < 0.05$ vs. the normal group. $^{\#\#}P < 0.01$, $^{\#\#\#}P < 0.005$ vs. the *P. acnes* group. HaCaT cells were randomly divided into the following six groups: normal, *P. acnes*, *P. acnes* + scrambled siRNA, *P. acnes* + Nrf2 siRNA3, *P. acnes* + PCT and *P. acnes* + PCT + Nrf2 siRNA3. **c** Western blot analysis was performed to detect HO-1 and NQO1 protein levels. Tubulin was used as the loading control. **d** Statistical analysis of the relative protein levels of HO-1 and NQO1. $^{*}P < 0.05$ vs. the normal group. $^{\#}P < 0.05$, $^{\#\#}P < 0.01$ vs. the *P. acnes* group. **e** ROS levels were measured with a DCFH-DA fluorescent probe and analysed by a ZOE fluorescent cell imager. The scale bar represents 100 μm.

necrosis factor (TNF)-induced NF-κB activation by downregulating NF-κB inhibitor alpha (IκBα) phosphorylation, p65 (a subunit of NF-κB) phosphorylation, p65 nuclear translocation and IκBα activation [5]. *P. acnes* upregulated p65 nuclear translocation, while PCT and JSH-23 displayed the opposite effect (Fig. 4a, b). Similarly, PCT and JSH-23 inhibited the *P. acnes*-induced secretion of TNF-α, IL-6 and IL-8 from HaCaT cells (Fig. 4c–e). The data suggested that PCT inhibited the *P. acnes*-induced inflammatory response by downregulating p65 nuclear translocation.

PCT Inhibits *P. Acnes*-Induced HaCaT Cell Proliferation and Migration by Upregulating Nrf2 and Downregulating p65

Finally, *P. acnes* induced HaCaT cell proliferation and migration, while PCT reversed these effects; moreover, the effect of PCT was downregulated by Nrf2 knockdown and p65 overexpression (Fig. 5a–d). The data suggested that PCT inhibited *P. acnes*-induced HaCaT cell proliferation and migration by upregulating Nrf2 and downregulating p65.

DISCUSSION

Currently, multiple therapeutic strategies for AV are available. However, each therapy has specific side effects. For example, retinoid therapy is complicated by some side effects, especially mucocutaneous toxicity [31], isotretinoin shows teratogenic effects [29]. In our study, PCT showed no toxicity against normal HaCaT cells (Fig. 1b). PCT is a naturally occurring hydroxylated analogue of resveratrol, displaying a wide spectrum of antioxidant, anti-inflammatory, anti-tumour and anti-angiogenic biological activities [3]. PCT has been found at low concentrations in various plants, including grapes, passion fruit, white tea, sugarcane and Japanese knotweed. Therefore, researchers

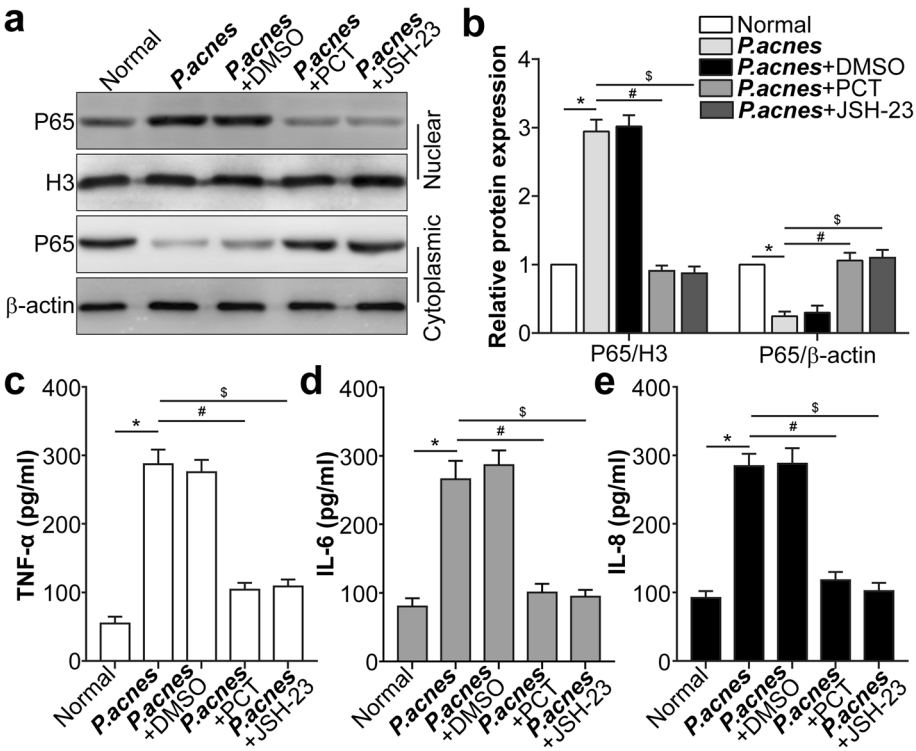

Fig. 4. PCT plays an anti-inflammatory role in *P. acnes*-challenged HaCaT cells. HaCaT cells were randomly divided into five groups: normal, *P. acnes*, *P. acnes* + DMSO, *P. acnes* + PCT and *P. acnes* + JSH-23. **a** Nuclear and cytoplasmic separation and Western blot analysis were performed to detect p65 subcellular location. H3 and β-actin were used as the nuclear and cytoplasmic loading controls, respectively. **b** Statistical analysis of the p65 relative protein level. $^{*}P < 0.05$ vs. the normal group; $^{\#}P < 0.05$ vs. the *P. acnes* group. TNF-α (**c**), IL-6 (**d**) and IL-8 (**e**) protein levels were measured by ELISA. $^{*}P < 0.05$ vs. the normal group. $^{\#}P < 0.05$ vs. the *P. acnes* group.

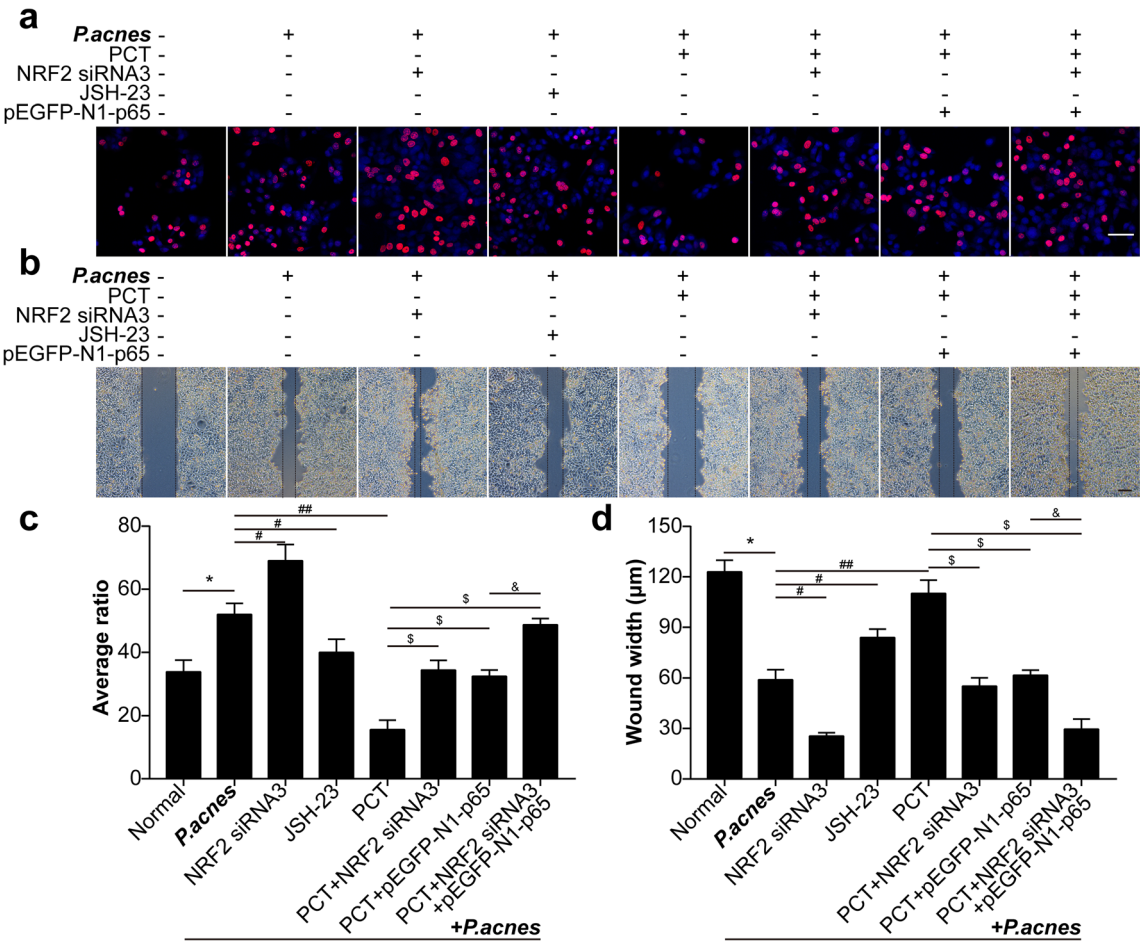

Fig. 5. PCT inhibits *P. acnes*-induced HaCaT cell proliferation and migration by upregulating Nrf2 and downregulating p65. HaCaT cells were randomly divided into the following eight groups: normal, *P. acnes*, *P. acnes* + Nrf2 siRNA3, *P. acnes* + JSH-23, *P. acnes* + PCT, *P. acnes* + Nrf2 siRNA3 + PCT, *P. acnes* + pEGFP-N1-p65 + PCT and *P. acnes* + Nrf2 siRNA3 + pEGFP-N1-p65 + PCT. **a** An EdU assay was performed to detect cell proliferation. **b** A scratch wound healing assay was performed to detect cell migration. **c** The average ratio of EdU-positive cells compared to DAPI-positive cells was calculated. **d** The wound width was calculated. $^{*}P < 0.05$ vs. the normal group; $^{\#}P < 0.05$, $^{\#\#}P < 0.05$ vs. the *P. acnes* group; $^{\$}P < 0.05$ vs. the *P. acnes* + PCT group in **c** and **d**. Scale bar = 100 μm in **a** and **b**.

have attempted to biosynthesize PCT from engineered microbial strains and have made marked progress [36]. Each gene involved in the biosynthetic pathways is well described; however, PCT production remains less than a few grams per litre. The reasons might be attributed to the optimization of each step in the biosynthetic pathway; for example, every metabolite, as well as each precursor, influences the ultimate product, PCT. In the future, PCT biosynthesis will be improved to meet the increasing need for PCT in basic and clinical applications.

PCT is an analogue of resveratrol, and sometimes the effect of PCT is stronger than that of resveratrol. Dimethylarginine dimethylaminohydrolase (DDAH) and arginase are regulators of endothelial NO synthase (eNOS). PCT acted similarly to resveratrol on the DDAH pathway but at 10-fold lower concentrations, indicating that PCT is more effective than resveratrol in restoring the DDAH expression and activity of endothelial cells under high-glucose oxidative stress [13]. Furthermore, PCT is a better peroxyl radical scavenger than is resveratrol [11]. Additionally, PCT and resveratrol can exert synergistic effects, strengthening their beneficial biological activities. For example, PCT and resveratrol inhibit inducible nitric oxide synthase (iNOS) expression and NF-κB activation in a mouse dextran sulfate sodium (DSS)-induced colitis model [40]. Thus, resveratrol-PCT hybrids have been biosynthesized to enhance their profitable effects [38].

Whether a resveratrol-PCT hybrid can alleviate HaCaT cell proliferation and migration requires further investigation.

The activation of the phosphoinositide-3-kinase (PI3K)/protein kinase B (AKT)/mechanistic target of rapamycin kinase (mTOR) pathway contributes to the proliferation of keratinocytes, as the inhibition of mTOR suppresses UVB-induced keratinocyte (HaCaT cell) proliferation and survival [7]. Additionally, apigenin inhibits UVB-induced mTOR signalling through the activation of AMP-activated protein kinase (AMPK). mTOR inhibition by apigenin enhances autophagy, further reducing the proliferation of keratinocytes (mouse 308 keratinocyte cell line) [6]. In the progression of acne, mTOR also plays vital positive roles. The nuclear expression of mTOR is obviously more intense in acne patients than in control subjects [1]. Moreover, mTOR increases Western diet (WD)-induced acne [30]. PCT inhibits the proliferation of prostate cancer cells by attenuating PI3K signalling and the phosphorylation of mTOR and AKT [17]. Therefore, we speculate that PCT inhibits the proliferation of HaCaT cells by downregulating the PI3K/AKT/mTOR pathway.

P. acnes activates the NLRP3 inflammasome in keratinocytes to produce pro-inflammatory cytokines such as interleukin-1β (IL-1β) and interleukin-18 (IL-18) [35]. Resveratrol plays an anti-inflammatory role by inhibiting the activation of the NLRP3 inflammasome under different pathological circumstances, including lipopolysaccharide (LPS)-induced acute lung injury [21], ionizing irradiation-induced inflammation in mesenchymal stem cells (MSCs) [14], and cerebral ischaemia/reperfusion injury in rats [16]. In our study, PCT played an anti-inflammatory role by inhibiting the activation of NF-κB and the secretion of pro-inflammatory cytokines. As an analogue of resveratrol, PCT might inhibit the *P. acnes*-induced activation of the NLRP3 inflammasome in keratinocytes.

In summary, PCT alleviates *P. acnes*-induced HaCaT cell proliferation and migration by inhibiting oxidative stress and the inflammatory response. Notably, there are some limitations to our study, such as the lack of the combined use of PCT and resveratrol and the absence of other mechanisms of the anti-inflammatory role of PCT, which requires further research. Our study reveals the functions of PCT in *P. acnes*-challenged HaCaT cells, supplying a novel therapeutic strategy for AV patients.

FUNDING INFORMATION

This study was partly supported by the National Science Foundation of China (no. 81560506, U1402223, 81460469 and 81760559).

COMPLIANCE WITH ETHICAL STANDARDS

Conflict of Interests. The authors declare that they have no conflict of interest.

REFERENCES

1. Agamia, N.F., D.M. Abdallah, O. Sorour, B. Mourad, and D.N. Younan. 2016. Skin expression of mammalian target of rapamycin and forkhead box transcription factor O1, and serum insulin-like growth factor-1 in patients with acne vulgaris and their relationship with diet. *The British Journal of Dermatology* 174 (6): 1299–1307. https://doi.org/10.1111/bjd.14409.
2. Ahn, J., Y.W. Chung, J.B. Park, and K.M. Yang. 2018. omega-hydroxyundec-9-enoic acid induces apoptosis by ROS mediated JNK and p38 phosphorylation in breast cancer cell lines. *Journal of Cellular Biochemistry* 119 (1): 998–1007. https://doi.org/10.1002/jcb.26267.
3. Akinwumi, B.C., K.M. Bordun, and H.D. Anderson. 2018. Biological activities of stilbenoids. *International Journal of Molecular Sciences* 19 (3). https://doi.org/10.3390/ijms19030792.
4. Alam, J., D. Stewart, C. Touchard, S. Boinapally, A.M. Choi, and J.L. Cook. 1999. Nrf2, a Cap'n'Collar transcription factor, regulates induction of the heme oxygenase-1 gene. *The Journal of Biological Chemistry* 274 (37): 26071–26078. https://doi.org/10.1074/jbc.274.37.26071.
5. Ashikawa, K., S. Majumdar, S. Banerjee, A.C. Bharti, S. Shishodia, and B.B. Aggarwal. 2002. Piceatannol inhibits TNF-induced NF-kappaB activation and NF-kappaB-mediated gene expression through suppression of IkappaBalpha kinase and p65 phosphorylation. *Journal of Immunology* 169 (11): 6490–6497. https://doi.org/10.4049/jimmunol.169.11.6490.
6. Bridgeman, B.B., P. Wang, B.P. Ye, J.C. Pelling, O.V. Volpert, and X. Tong. 2016. Inhibition of mTOR by apigenin in UVB-irradiated keratinocytes: a new implication of skin cancer prevention. *Cellular Signalling* 28 (5): 460–468. https://doi.org/10.1016/j.cellsig.2016.02.008.
7. Carr, T.D., J. DiGiovanni, C.J. Lynch, and L.M. Shantz. 2012. Inhibition of mTOR Suppresses UVB-Induced Keratinocyte Proliferation and Survival. *Cancer Prevention Research* 5 (12): 1394–1404. https://doi.org/10.1158/1940-6207.Capr-12-0272-T.
8. Chartoumpekis, D.V., N. Wakabayashi, and T.W. Kensler. 2015. Keap1/Nrf2 pathway in the frontiers of cancer and non-cancer cell metabolism. *Biochemical Society Transactions* 43 (4): 639–644. https://doi.org/10.1042/BST20150049.
9. Choi, K.H., J.E. Kim, N.R. Song, J.E. Son, M.K. Hwang, S. Byun, J.H. Kim, K.W. Lee, and H.J. Lee. 2010. Phosphoinositide 3-kinase is a novel target of piceatannol for inhibiting PDGF-BB-induced

proliferation and migration in human aortic smooth muscle cells. *Cardiovascular Research* 85 (4): 836–844. https://doi.org/10.1093/cvr/cvp359.

10. Cong, T.X., D. Hao, X. Wen, X.H. Li, G. He, and X. Jiang. 2019. From pathogenesis of acne vulgaris to anti-acne agents. *Archives of Dermatological Research* 311 (5): 337–349. https://doi.org/10.1007/s00403-019-01908-x.
11. Cordova-Gomez, M., A. Galano, and J.R. Alvarez-Idaboy. 2013. Piceatannol, a better peroxyl radical scavenger than resveratrol. *RSC Advances* 3 (43): 20209–20218. https://doi.org/10.1039/c3ra42923g.
12. Das, S., and R.V. Reynolds. 2014. Recent advances in acne pathogenesis: implications for therapy. *American Journal of Clinical Dermatology* 15 (6): 479–488. https://doi.org/10.1007/s40257-014-0099-z.
13. Frombaum, M., P. Therond, R. Djelidi, J.L. Beaudeux, D. Bonnefont-Rousselot, and D. Borderie. 2011. Piceatannol is more effective than resveratrol in restoring endothelial cell dimethylarginine dimethylaminohydrolase expression and activity after high-glucose oxidative stress. *Free Radical Research* 45 (3): 293–302. https://doi.org/10.3109/10715762.2010.527337.
14. Fu, Y., Y. Wang, L. Du, C. Xu, J. Cao, T. Fan, J. Liu, et al. 2013. Resveratrol inhibits ionising irradiation-induced inflammation in MSCs by activating SIRT1 and limiting NLRP-3 inflammasome activation. *International Journal of Molecular Sciences* 14 (7): 14105–14118. https://doi.org/10.3390/ijms140714105.
15. Grange, P.A., C. Chereau, J. Raingeaud, C. Nicco, B. Weill, N. Dupin, and F. Batteux. 2009. Production of superoxide anions by keratinocytes initiates P. acnes-induced inflammation of the skin. *PLoS Pathogens* 5 (7): e1000527. https://doi.org/10.1371/journal.ppat.1000527.
16. He, Q., Z. Li, Y. Wang, Y. Hou, L. Li, and J. Zhao. 2017. Resveratrol alleviates cerebral ischemia/reperfusion injury in rats by inhibiting NLRP3 inflammasome activation through Sirt1-dependent autophagy induction. *International Immunopharmacology* 50: 208–215. https://doi.org/10.1016/j.intimp.2017.06.029.
17. Hsieh, T.C., C.Y. Lin, H.Y. Lin, and J.M. Wu. 2012. AKT/mTOR as novel targets of polyphenol piceatannol possibly contributing to inhibition of proliferation of cultured prostate cancer cells. *ISRN Urology* 2012: 272697. https://doi.org/10.5402/2012/272697.
18. Hur, K.Y., S.H. Kim, M.A. Choi, D.R. Williams, Y.H. Lee, S.W. Kang, U.C. Yadav, S.K. Srivastava, M. Jung, J.W. Cho, S.G. Kim, E.S. Kang, E.J. Lee, and H.C. Lee. 2010. Protective effects of magnesium lithospermate B against diabetic atherosclerosis via Nrf2-ARE-NQO1 transcriptional pathway. *Atherosclerosis* 211 (1): 69–76. https://doi.org/10.1016/j.atherosclerosis.2010.01.035.
19. Jahns, A.C., B. Lundskog, R. Ganceviciene, R.H. Palmer, I. Golovleva, C.C. Zouboulis, A. McDowell, S. Patrick, and O.A. Alexeyev. 2012. An increased incidence of Propionibacterium acnes biofilms in acne vulgaris: a case-control study. *The British Journal of Dermatology* 167 (1): 50–58. https://doi.org/10.1111/j.1365-2133.2012.10897.x.
20. Jahns, A.C., H. Eilers, R. Ganceviciene, and O.A. Alexeyev. 2015. Propionibacterium species and follicular keratinocyte activation in acneic and normal skin. *The British Journal of Dermatology* 172 (4): 981–987. https://doi.org/10.1111/bjd.13436.
21. Jiang, L., L. Zhang, K. Kang, D. Fei, R. Gong, Y. Cao, S. Pan, M. Zhao, and M. Zhao. 2016. Resveratrol ameliorates LPS-induced acute lung injury via NLRP3 inflammasome modulation. *Biomedicine & Pharmacotherapy* 84: 130–138. https://doi.org/10.1016/j.biopha.2016.09.020.
22. Kistowska, M., S. Gehrke, D. Jankovic, K. Kerl, A. Fettelschoss, L. Feldmeyer, G. Fenini, A. Kolios, A. Navarini, R. Ganceviciene, J. Schauber, E. Contassot, and L.E. French. 2014. IL-1beta drives inflammatory responses to propionibacterium acnes in vitro and in vivo. *The Journal of Investigative Dermatology* 134 (3): 677–685. https://doi.org/10.1038/jid.2013.438.
23. Kita, Y., Y. Miura, and K. Yagasaki. 2012. Antiproliferative and anti-invasive effect of piceatannol, a polyphenol present in grapes and wine, against hepatoma AH109A cells. *Journal of Biomedicine and Biotechnology*. https://doi.org/10.1155/2012/672416.
24. Ko, Y.J., H.H. Kim, E.J. Kim, Y. Katakura, W.S. Lee, G.S. Kim, and C.H. Ryu. 2013. Piceatannol inhibits mast cell-mediated allergic inflammation. *International Journal of Molecular Medicine* 31 (4): 951–958. https://doi.org/10.3892/ijmm.2013.1283.
25. Kobayashi, M., and M. Yamamoto. 2005. Molecular mechanisms activating the Nrf2-Keap1 pathway of antioxidant gene regulation. *Antioxidants & Redox Signaling* 7 (3-4): 385–394. https://doi.org/10.1089/ars.2005.7.385.
26. Liu, D., D.H. Kim, J.M. Park, H.K. Na, and Y.J. Surh. 2009. Piceatannol inhibits phorbol ester-induced NF-kappa B activation and COX-2 expression in cultured human mammary epithelial cells. *Nutrition and Cancer* 61 (6): 855–863. https://doi.org/10.1080/01635580903285080.
27. Maruki-Uchida, H., I. Kurita, K. Sugiyama, M. Sai, K. Maeda, and T. Ito. 2013. The protective effects of piceatannol from passion fruit (Passiflora edulis) seeds in UVB-irradiated keratinocytes. *Biological & Pharmaceutical Bulletin* 36 (5): 845–849. https://doi.org/10.1248/bpb.b12-00708.
28. Melnik, B.C. 2018. Acne vulgaris: the metabolic syndrome of the pilosebaceous follicle. *Clinics in Dermatology* 36 (1): 29–40. https://doi.org/10.1016/j.clindermato1.2017.09.006.
29. Melnik, B.C. 2018. Overexpression of p53 explains isotretinoin's teratogenicity. *Experimental Dermatology* 27 (1): 91–93. https://doi.org/10.1111/exd.13420.
30. Melnik, B.C., and C.C. Zouboulis. 2013. Potential role of FoxO1 and mTORC1 in the pathogenesis of Western diet-induced acne. *Experimental Dermatology* 22 (5): 311–315. https://doi.org/10.1111/exd.12142.
31. Mirnezami, M., and H. Rahimi. 2018. Is Oral Omega-3 Effective in Reducing Mucocutaneous Side Effects of Isotretinoin in Patients with Acne Vulgaris? *Dermatology Research and Practice* 2018: 6974045. https://doi.org/10.1155/2018/6974045.
32. Puhvel, S.M., M. Barfatani, M. Warnick, and T.H. Sternberg. 1964. Study of antibody levels to corynebacterium acnes. in the serum of patients with acne vulgaris, using bacterial agglutination, agar gel immunodiffusion, and immunofluorescence techniques. *Archives of Dermatology* 90: 421–427. https://doi.org/10.1001/archderm.1964.01600040049011.
33. Son, Y., S.J. Byun, and H.O. Pae. 2013. Involvement of heme oxygenase-1 expression in neuroprotection by piceatannol, a natural analog and a metabolite of resveratrol, against glutamate-mediated oxidative injury in HT22 neuronal cells. *Amino Acids* 45 (2): 393–401. https://doi.org/10.1007/s00726-013-1518-9.
34. Song, H., J.I. Jung, H.J. Cho, S. Her, S.H. Kwon, R. Yu, Y.H. Kang, K.W. Lee, and J.H.Y. Park. 2015. Inhibition of tumor progression by oral piceatannol in mouse 4T1 mammary cancer is associated with decreased angiogenesis and macrophage infiltration. *Journal of Nutritional Biochemistry* 26 (11): 1368–1378. https://doi.org/10.1016/j.jnutbio.2015.07.005.
35. Suh, D.H., and H.H. Kwon. 2015. What's new in the physiopathology of acne? *The British Journal of Dermatology* 172 (Suppl 1): 13–19. https://doi.org/10.1111/bjd.13634.
36. Sun, X., X. Shen, R. Jain, Y. Lin, J. Wang, J. Sun, J. Wang, Y. Yan, and Q. Yuan. 2015. Synthesis of chemicals by metabolic engineering

of microbes. *Chemical Society Reviews* 44 (11): 3760–3785. https://doi.org/10.1039/c5cs00159e.

37. Tang, Q., Z. Feng, M. Tong, J. Xu, G. Zheng, L. Shen, P. Shang, Y. Zhang, and H. Liu. 2017. Piceatannol inhibits the IL-1beta-induced inflammatory response in human osteoarthritic chondrocytes and ameliorates osteoarthritis in mice by activating Nrf2. *Food & Function* 8 (11): 3926–3937. https://doi.org/10.1039/c7fo00822h.
38. Vo, D.D., and M. Elofsson. 2016. Total synthesis of viniferifuran, resveratrol-piceatannol hybrid, anigopreissin A and analogues - investigation of demethylation strategies. *Advanced Synthesis & Catalysis* 358 (24): 4085–4092. https://doi.org/10.1002/adsc.201601089.
39. Wang, Y.Y., A.R. Ryu, S. Jin, Y.M. Jeon, and M.Y. Lee. 2017. Chlorin e6-mediated photodynamic therapy suppresses P. acnes-induced inflammatory response via NFkappaB and MAPKs signaling pathway. *PLoS One* 12 (1): e0170599. https://doi.org/10.1371/journal.pone.0170599.
40. Youn, J., J.S. Lee, H.K. Na, J.K. Kundu, and Y.J. Surh. 2009. Resveratrol and piceatannol inhibit iNOS expression and NF-kappa B activation in dextran sulfate sodium-induced mouse colitis. *Nutrition and Cancer-an International Journal* 61 (6): 847–854. https://doi.org/10.1080/01635580903285072.
41. Zhai, J., J. Shen, G. Xie, J. Wu, M. He, L. Gao, Y. Zhang, X. Yao, and L. Shen. 2019. Cancer-associated fibroblasts-derived IL-8 mediates resistance to cisplatin in human gastric cancer. *Cancer Letters* 454: 37–43. https://doi.org/10.1016/j.canlet.2019.04.002.
42. Zouboulis, C. 2019. Neuroendocrinology of Acne Vulgaris. *Acta Dermato-Venereologica* 99 (8): 739–739.